

# Phương pháp định vị sự cố dựa trên truyền sóng một đầu sử dụng biến đổi wavelet rời rạc

## TÓM TẮT

Định vị sự cố là một trong những phương pháp hiệu quả để nâng cao độ tin cậy và giảm thiểu thời gian khắc phục sự cố của hệ thống điện. Hai phương pháp chính bao gồm phương pháp dựa trên tổng trỏ và phương pháp dựa trên truyền song đã được phát triển để định vị sự cố trên đường dây tải điện. Các phương pháp định vị sự cố dựa trên truyền song sử dụng đặc tính của quá trình lan truyền song để xác định thời điểm đến của các sóng phản xạ và sóng truyền tới tại các điểm đầu của đường dây. Khoảng cách từ đầu đường dây đến điểm sự cố có thể được tính toán. Bài báo này phát triển một phương pháp định vị sự cố mới dựa trên kỹ thuật truyền sóng sử dụng biến đổi wavelet rời rạc (DWT). Dữ liệu đo lường dòng điện sự cố tại các đầu đường dây sẽ được chuyển đổi sang hệ  $\alpha\beta0$  bằng biến đổi Clark, thành phần dòng điện alpha sẽ được phân tích bởi biến đổi DWT để trích xuất các hệ số chi tiết có hàm chứa các thành phần tần số bậc cao. Do vậy quá trình lùn truyền sóng sẽ xuất hiện trên đường dây sau khi ngắn mạch xảy ra ở bất kỳ vị trí nào dọc theo chiều dài đường dây. Kỹ thuật định vị sự cố dựa trên phương pháp truyền sóng một đầu được nghiên cứu trong bài báo này cho một hệ thống điện có một đường dây mạch đơn. Sự lựa chọn tần số lấy mẫu phù hợp để định vị sự cố trên đường dây truyền tải cũng được khảo sát để đạt được độ chính xác cao hơn. Các kết quả nghiên cứu được mô phỏng và kiểm chứng bằng phần mềm MATLAB/Simulink.

**Từ khóa:** Đường dây truyền tải, sai số ước lượng, định vị sự cố, phương pháp truyền sóng, biến đổi wavelet rời rạc.

# A fault location method based on single-ended travelling wave using discrete wavelet transform

## ABSTRACT

Fault location is one of the most efficient methods to improve reliability and to reduce downtime of a power system. For this, two main methods including the impedance and travelling wave approaches have been developed for locating fault on power transmission lines. The travelling wave-based fault location methods use the characteristics of travelling wave propagation to determine the arrival times of the reflected and forward waves at the ends of the transmission line. The distance from the line end to the fault can be calculated. This paper developed a new fault location method based on the travelling wave using the discrete wavelet transform (DWT). The fault current measurement data at the two line ends is converted to the  $\alpha\beta0$  frame via the Clark transform, the alpha current component is then decomposed by the DWT to extract the detail coefficients containing the high frequency levels. Thus the travelling wave propagation will appear on the transmission line after a fault occurs at any location along the line. The single-ended technique is considered in this paper for a test system based on a single-circuit power transmission line model. The choice of the most suitable sampling frequency for locating faults in transmission lines was also investigated to achieve a high fault location accuracy. The research results are simulated and verified in MATLAB/Simulink software.

**Keywords:** *Transmission line, estimation error, fault location, travelling wave method, discrete wavelet transform.*

## 1. INTRODUCTION

In power system operation processing, short circuits are very extremely serious, they occur randomly that people can not diagnose their occurrence. Additionally, because a power transmission line often spreads on widely areas and crosses over hilly regions with a high density of lightning strikes, the transmission line is an element which suffers most short circuits in a power system<sup>1</sup>. With the complicated topographic of hilly regions, the fault detection, identification and location technique requires a high accuracy to create quick and convenient conditions in finding and restoring the power system. As a result, the power system can be improved reliability and reduced downtime<sup>2</sup>.

In power systems, four typical types of fault consist of the three-phase-to-ground (ABCG), single-phase-to-ground (AG, BG, CG), phase-to-phase (AB, BC, AC), and double-phase-to-ground (ABG, BCG, ACG) faults as shown in Figure 1. The fault location system need to detect and identify accurately the fault type before it can locate the fault in the transmission line. Therefore, the fault locator uses the three phase fault current characteristics to identify exactly the fault type<sup>3</sup>.

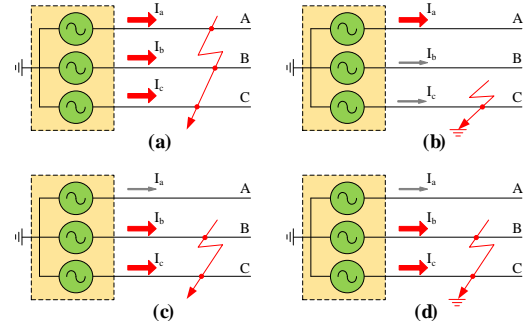


**Figure 1.** Fault types: (a) Three-phase-to-ground fault, (b) Single-phase-to-ground fault, (c) Phase-to-phase fault, (d) Double-phase-to-ground fault.

For the fault location on power transmission lines, distance information from the relay to the fault location recorded by the digital distance relay can be applied to determine the fault location. However the information has a high estimation error, the manual finding way need to be applied for supporting on the whole power transmission line. Thus this method can not find and restore quickly and accurately the fault on transmission line as well as not have economical save<sup>4</sup>. From the aforementioned issues, it can be necessarily recognized that the fault detection, identification and location on power transmission lines is an extremely important problem to bring a high effectiveness in power system operation.

The studies on the fault location on power transmission lines can be mainly divided into two groups, including the impedance and travelling wave methods as shown in Figure 2. The impedance-based fault location methods have some advantages such as the simply integration into the central control unit of the power system<sup>5-8</sup>. However its disadvantage is the significant dependance on the fault resistance while the travelling wave-based methods have a high accuracy and does not depend on the fault resistance<sup>9-14</sup>.

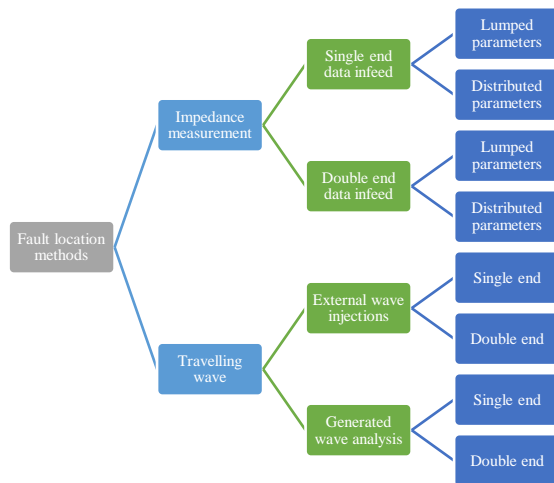


**Figure 2.** Two main fault location methods<sup>3</sup>.

In the published work<sup>11</sup>, the fault location based on travelling wave time-frequency characteristics was proposed to determine the fault location from a single end of the transmission line. The novel travelling wave-based fault location method for overhead power transmission lines which formed the complete theoretical analysis of the distortion phenomenon of travelling wave signal and the the improved travelling wave fault location method considering distortion phenomenon was studied in the publication<sup>12</sup>. The fault locator based on the travelling wave method for high impedance events was implemented for the Brazilian transmission companies<sup>13</sup>. The frequency-dependent characteristics of high-voltage alternating current (HVAC) transmission lines was researched to propose a travelling wave-based fault location system<sup>14</sup>. As a result, the paper focuses on the fault location methods based on travelling wave.

Two main travelling wave-based fault location methods consist of the single- and double- ended methods. For single-ended methods, voltage and current waves measured and recorded at on end of the transmission line will be used to determine for fault location<sup>15, 16</sup>. For double-ended methods, both of voltage and

current waves measured and recorded at two ends of the transmission line will applied in the fault location system, therefore the measurement data need to be synchronized<sup>17-20</sup>. A wavelet transform (WT) is the decomposition of a signal into a set of basis functions consisting of contractions, expansions, and translation of a mother wavelet. Wavelet transforms are mathematical tools for analyzing data where features vary over different time-frequency scales, therefore they have been widely applied in many travelling wave-based fault location systems on power transmission lines<sup>21, 22</sup>.

From above analysis, it can be be observed that there are still gaps about the travelling wave-based fault location method, therefore this paper focuses to study and propose a new fault location method based on travelling wave using the discrete wavelet transform (DWT). Some different wavelet mothers were considered to evaluate the estimation effectiveness in fault location. The arrival current times at the ends of the transmission line are extracted from the detail coefficients by using the DWT. Additionally, single-ended method was applied for a single-circuit transmission line which was modeled and simulated in MATLAB/Simulink software to record the voltage and current waves at a two ends of the line. Besides, the different fault resistances and locations were varied along the transmission line to create many case studies in this paper. The main outstanding contributions of this paper are summarized as follows: (i) Developing the travelling wave-based fault location method using the DWT to extract the arrival times at the line ends and determine the fault location on the transmission line. Additionally, some mother wavelets including ‘db4’, ‘coif4’, and ‘sym4’ are considered to verify their effectiveness for fault location, (ii) Changing the sampling frequency of the current signal as well as the fault resistance to record the measurement data and applying the proposed method to calculate the fault location on the power transmission line, and (iii) Applying MATLAB/Simulink software for modeling and simulating the typical single-circuit transmission line to assume many fault locations along the line.

The next parts of this paper are structured as follows: The proposed method for fault location based on travelling wave using wavelet transform is presented in Section 2. In Section 3, some case studies for the single-circuit transmission line are modeled and simulated in MATLAB/Simulink software to verify and evaluate the proposed

method. Finally, some conclusions is reached in Section 4.

## 2. PROPOSED METHOD

### 2.1. Travelling wave technique

In general, when a fault occurs on the transmission line at the time that the voltage is not equal zero, it will form propagation waves along the line. These waves will propagate from the fault location to the two line ends at the propagation speed approximately the light speed<sup>4</sup>. A transmission line can be modeled by its parameters including the series resistance  $R$ , the series inductance  $L$ , the shunt conductance  $G$ , and the shunt capacitance  $C$ . For a  $dx$ -segment of a transmission line, the constant parameters are  $Rdx$ ,  $Gdx$ ,  $Ldx$  and  $Cdx$  as shown in Figure 3.

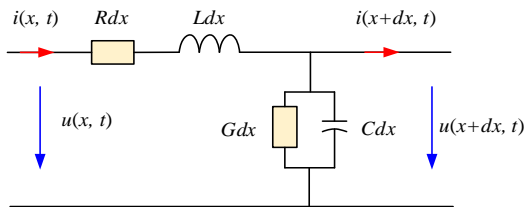


**Figure 3.** Single-phase transmission line model of distributed parameters.

The travelling wave can be determined as the solutions of the linear differential equations for the transmission line. For the general transmission line, the partial differential equations represent for the voltage and current of the line as follows<sup>19, 20</sup>:

$$\frac{\partial u(x, t)}{\partial x} = -Ri(x, t) - L \frac{\partial i(x, t)}{\partial t} \quad (1)$$

$$\frac{\partial i(x, t)}{\partial x} = -Gu(x, t) - C \frac{\partial u(x, t)}{\partial t} \quad (2)$$

For the lossless transmission line, the partial differential equations that describe the voltage and current of the line can be rewritten as follows<sup>21</sup>:

$$\frac{\partial u(x, t)}{\partial x} = -L \frac{\partial i(x, t)}{\partial t} \quad (3)$$

$$\frac{\partial i(x, t)}{\partial x} = -C \frac{\partial u(x, t)}{\partial t} \quad (4)$$

The voltage and current solutions of the above partial differential equations in the time domain can be satisfied by the general forms as follows<sup>21</sup>:

$$u(x, t) = A_1 \left( t + \frac{x}{v} \right) + A_2 \left( t - \frac{x}{v} \right) \quad (5)$$

$$i(x, t) = \frac{1}{Z_0} \left[ A_1 \left( t + \frac{x}{v} \right) - A_2 \left( t - \frac{x}{v} \right) \right] \quad (6)$$

where  $Z_0 = \sqrt{L/C}$  is the characteristic impedance of the lossless line;  $A_1 \left( t + \frac{x}{v} \right)$  and  $A_2 \left( t - \frac{x}{v} \right)$  is the reflected and forward travelling wave, respectively.

The propagation speed of the travelling wave along the transmission line is impacted by the line characteristics of inductance ( $L$ ) and capacitance ( $C$ ). This relationship can be seen in the following equation<sup>9</sup>:

$$v_{prop} = \frac{1}{\sqrt{LC}} \quad (7)$$

The travelling wave methods use the timing to locate the fault in the transmission line. The two travelling wave methods including single- and double- ended methods are applied as shown in Figure 4. The single-ended travelling wave-based fault location method uses the propagation velocity ( $v_{prop}$ ), but not the line's length ( $L_{line}$ ). This method is based on the travelling wave's reflections from the lattice diagram in Figure 4(a). The fault location can be determined by using the difference between the fault's arrival time and the first reflection's arrival time. For this method, the fault location ( $X$ ) are calculated as follows:

$$X = \frac{1}{2} [(t_{A2} - t_A)v_{prop}] \quad (8)$$

The double-ended travelling wave-based fault location records the arrival time of the travelling wave at the each line end and also use the propagation velocity ( $v_{prop}$ ), the line's length ( $L_{line}$ ) and the difference time between the arrival times to locate the fault as shown in Figure 4(b). Therefore, this method requires the communication between the two relays at the two line ends. According to this method, the fault location ( $X$ ) is determined as follows:

$$X = \frac{1}{2} [L_{line} + (t_A - t_B)v_{prop}] \quad (9)$$

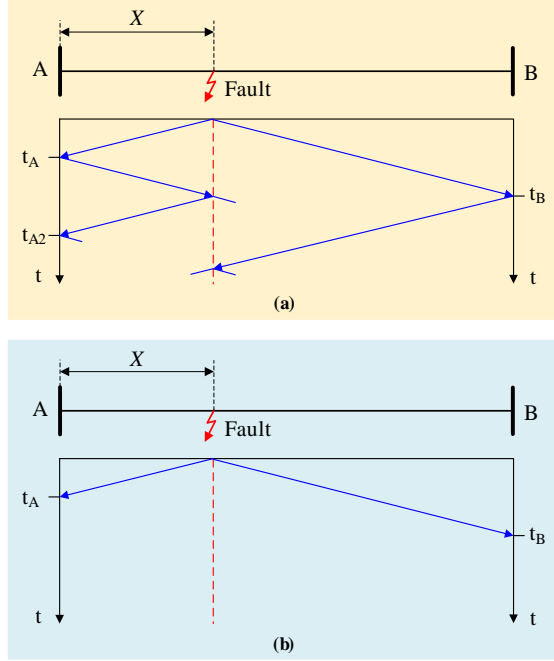


**Figure 4.** Basic visualization of travelling wave-based fault location methods: **(a)** Single-ended method, **(b)** Double-ended method<sup>9</sup>.

## 2.2. Discrete wavelet transform

Discrete wavelet transform (DWT) is a discrete form of continuous wavelet transform (CWT)<sup>23</sup>. The CWT of a continuous signal in time domain is defined as follows:

$$CWT(a, b) = \int_{-\infty}^{+\infty} f(t) \psi_{a,b}^*(t) dt, \quad (10)$$

$a, b \in R, a \neq 0$

$$\text{with: } \psi_{a,b}^*(t) = \frac{1}{\sqrt{|a|}} \psi^* \left( \frac{t-b}{a} \right) \quad (11)$$

where  $\psi(t)$  is the mother wavelet; the symbol “\*” represents for a complex number;  $a$  and  $b$  are scale and transition coefficients, respectively. The scale coefficient  $a$  is used to establish the frequency variation and wavelet length; the transition coefficient  $b$  is used for describing the signal transiting location.

In practical applications, the DWT is used to replace the CWT. This way is performed using the discrete values  $a = a_0^m$  and  $b = nb_0a_0^m$  to replace the scale and transition coefficients. Thus, the following equation is established:

$$\psi_{m,n}(k) = a_0^{-\frac{m}{2}} \psi(a_0^{-m}k - nb_0), \quad (12)$$

$m, n \in Z$

where  $m$  and  $n$  represent for the frequency and time locations. In general,  $a_0 = 2$  and  $b_0 = 1$  are set to create an orthogonal wavelet transform and multi-resolution analysis.

In multi-resolution analysis, the signal  $f(k)$  is decomposed into the approximation and detail coefficients which are performed by the scale functions  $\phi_{m,n}(k)$  and the wavelets  $\psi_{m,n}(k)$ :

$$\phi_{m,n}(k) = 2^{-(m/2)} \phi(2^{-m}k - n) \quad (13)$$

$$\psi_{m,n}(k) = 2^{-(m/2)} \psi(2^{-m}k - n) \quad (14)$$

The scale functions is related to the low-pass filters with the filtering factors  $\{g(n)\}$  and the wavelet is related to the high-pass filters with the filtering factors  $\{h(n)\}$ . These relationships are displayed as follows:

$$\phi(k) = \sqrt{2} \sum_n g(n) \phi(2k - n) \quad (15)$$

$$\psi(k) = \sqrt{2} \sum_n h(n) \phi(2k - n) \quad (16)$$

The above filters have some following important characteristics:

$$\sum_n g^2(n) = 1 \quad (17)$$

$$\sum_n h^2(n) = 1 \quad (18)$$

$$\sum_n g(n) = \sqrt{2} \quad (19)$$

$$\sum_n h(n) = \sqrt{2} \quad (20)$$

The filter  $h(n)$  is an other type of the filter  $g(n)$  and there is an odd integer  $N$  which satisfies the following equation:

$$h(n) = (-1)^n g(N - 1 - n) \quad (21)$$

The significant advantage of the DWT is to have the changeable window length, therefore it has a high resolution in time-frequency domain for all frequency ranges<sup>21-23</sup>. As a result, the DWT can be applied for the travelling wave-based fault location method. To process signals using the DWT, this work applies some available functions in MATLAB toolbox. The function **wavedec** will give the wavelet decompositions of the input

signal  $x$  at the level  $n$  with the mother wavelet ‘wname’ as follows:

$$[c, l] = \text{wavedec}(x, n, 'wname') \quad (22)$$

The function **detcoef** is applied to determine the detail coefficients from the outputs  $c$  and  $l$  at the level  $n$  as follows:

$$D = \text{detcoef}(c, l, n) \quad (23)$$

The detail coefficient characteristics in Eq. (23) as shown in Figure 5 are used to detect and calculate the fault location on the transmission line based on the travelling wave theory.

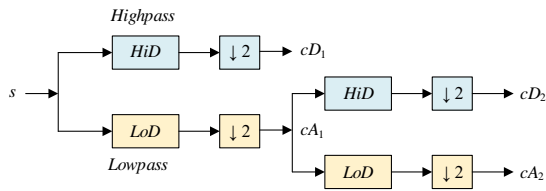


Figure 5. Filter bank using wavedec function.

### 2.3. Clarke transform

The Clarke transform is a signal processing technique to convert the initial signal in the  $abc$  frame into the  $\alpha\beta\theta$  frame as follows<sup>24</sup>. In this paper, the alpha aerial mode is used for fault location on a transmission line in this paper.

$$\begin{bmatrix} I_\alpha \\ I_\beta \\ I_0 \end{bmatrix} = \frac{2}{3} \begin{bmatrix} 1 & -\frac{1}{2} & -\frac{1}{2} \\ 0 & \frac{\sqrt{3}}{2} & -\frac{\sqrt{3}}{2} \\ \frac{1}{2} & \frac{1}{2} & \frac{1}{2} \end{bmatrix} \begin{bmatrix} I_a \\ I_b \\ I_c \end{bmatrix} \quad (24)$$

## 3. SIMULATED CASE STUDIES

### 3.1. Test system description

The proposed method is verified and evaluated in this section by applying to two case studies including the single- and double- circuit transmission lines. These two three-phase transmission lines are modeled and simulated in MATLAB/Simulink software to validate the effectiveness of the fault location method based on travelling wave using the DWT. Many different fault resistances and locations along the transmission line are created to record the voltage and current waveforms at the two line ends. The sampling frequency is also set at many levels to get the simulation data. Additionally, the estimation error for comparing the effectiveness of the case studies is calculated as the following equation<sup>6</sup>.

$$\text{Error}(\%) = \left| \frac{L_{\text{estimate}} - L_{\text{actual}}}{L} \right| 100 \quad (25)$$

where  $L_{\text{actual}}$  is the actual line segment length from the line end to the fault location,  $L_{\text{estimate}}$  is the distance from the line end to the fault location which is estimated by the proposed method; and  $L$  is the line length.

The case studies are simulated via MATLAB/Simulink software according to the test system single-line diagram as shown in Figure 6. In the test system, the main element parameters are as follows. The three-phase source A has the phase-to-phase nominal voltage of 220 kV, the nominal frequency of 50 Hz; the inner resistance of 0.8929  $\Omega$ ; and the inner inductance of 16.58 mH. The three-phase source B has the phase-to-phase nominal voltage of 220 kV, the nominal frequency of 50 Hz; the inner resistance of 0.9375  $\Omega$ ; and the inner inductance of 17.41 mH; and the 100 km distributed parameters line has the positive- and zero- sequence resistances of 0.01273  $\Omega/\text{km}$  and 0.3864  $\Omega/\text{km}$ , respectively; the positive- and zero- sequence inductances of 0.9337 mH/km and 4.1264 mH/km, respectively; the positive- and zero- sequence capacitances of 0.01274  $\mu\text{F}/\text{km}$  and 0.007751  $\mu\text{F}/\text{km}$ , respectively. Additionally, the fault block can be added to the middle position of the distributed parameter line to create different types of fault on the power transmission line.

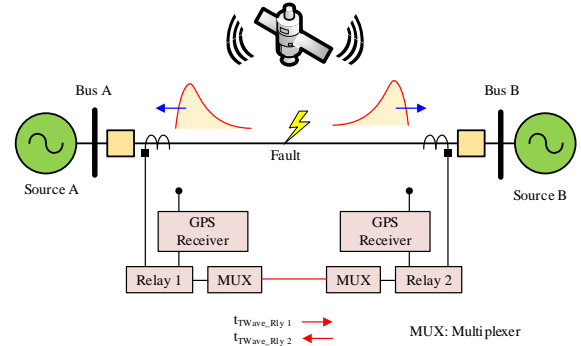
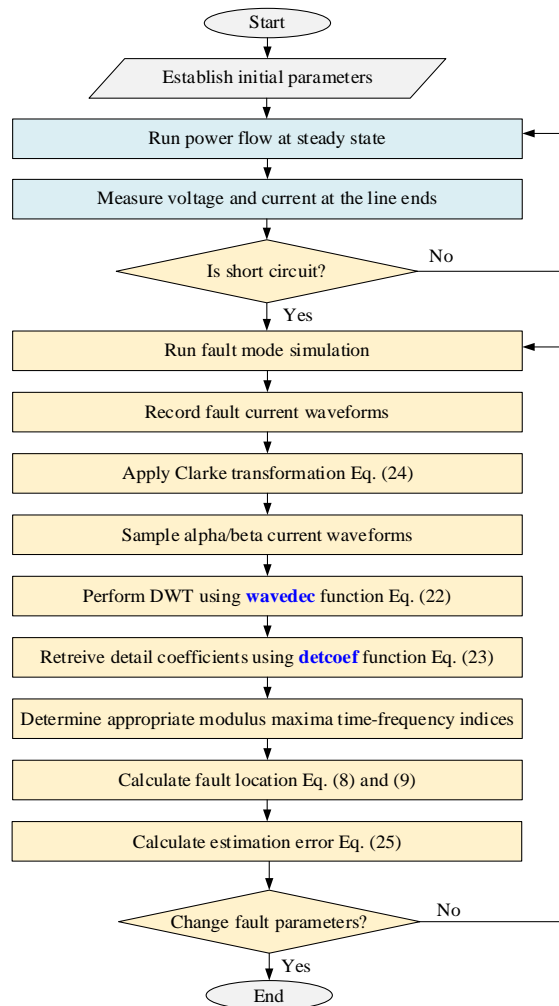


Figure 6. Test system single-line diagram.

The proposed algorithm flowchart for performing the simulation results in this paper is presented in Figure 7. As shown in this figure, there are two main periods including the steady state simulation and fault mode simulation for the test systems. After establishing all the initial parameters for the test system, the algorithm will run power flow at the steady state to get the voltage and current measurements at the power transmission line ends. A short circuit is created on the line and the test system is then simulated to record the fault current waveforms at the line

ends. The Clarke transformation is applied using Eq. (24) to transform the fault current from the  $abc$  framework to  $\alpha\beta0$  framework. The alpha aerial mode will be sampled at various sampling frequency to perform the DWT using **wavedec** function Eq. (22). After that, Equation (23) is used to retrieve the detail coefficients using the function **detcoef**. The level-1 detail coefficient is applied to extract the maxima time-frequency indices and calculate the fault location using Eq. (8)-(9) and the estimation error using Eq. (25). In the proposed algorithm flowchart, the fault type, resistance, and location can be randomly changed to verify the effectiveness of the proposed fault location method based on travelling wave using the DWT.



**Figure 7.** Proposed flowchart based on DWT.

The test power system modeled in MATLAB/Simulink software is shown in Figure 8. The continuous simulation mode is performed for all case studies in this paper. The fault current waveform at Source A is sampled at various sampling frequency to create simulation data for verifying the proposed fault location method.

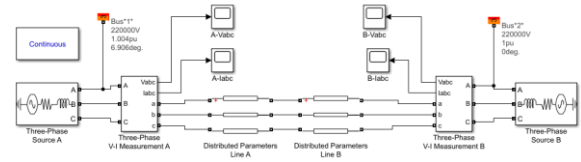


**Figure 8.** Single-circuit transmission line model in MATLAB/Simulink.

### 3.2. Pre-fault mode

At the pre-fault steady state, it is assumed that the three-phase source A is generating a active power of 200 MW transmitting through the transmission line to the three-phase source B which are considered as the swing bus in the test system. Power flow problem is performed at this mode to collect the initial measurement data including the voltage of Source A ( $\dot{U}_A = 1.004\angle6.9^\circ$  pu) and the voltage of Source B ( $\dot{U}_B = 1.00\angle0^\circ$  pu). The three-phase voltage and current waveforms at the beginning of the line are simulated in the total simulation time of 10 cycles (or 0.2 seconds) as shown in Figure 9. From these simulation results, it can be observed that at the pre-fault steady state the three-phase voltage phasors as well as the three-phase current phasors are balance. Additionally, the current measurement of 524 A can be determined from these current waveform. This steady state is considered the initial mode for investigating various fault modes which occur at various fault resistances and locations along the power transmission line.

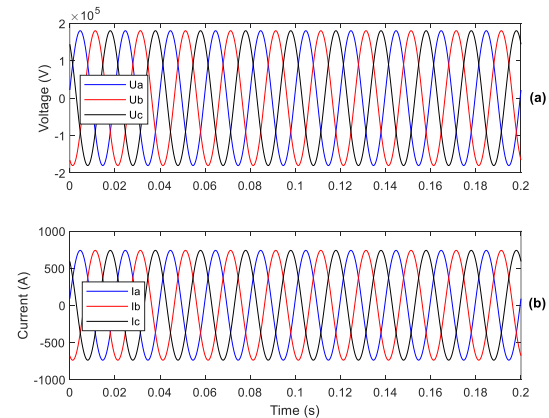


**Figure 9.** Pre-fault simulation results at Source A: (a) Voltage waveform, (b) Current waveform.

### 3.3. Fault modes

A single-phase-to-ground fault (AG) is assumed that it occurs at the time  $t = 0.1$  sec. The fault appears at the location far away Source A of 20 km with a fault resistance of  $1 \Omega$ . The total simulation time is set by 0.2 sec. The three-phase

*abc* voltage waveform (Figure 10a) and three-phase *abc* current waveform (Figure 10b), and the  $\alpha\beta0$  current waveform (Figure 10c). It can be obviously that after occurring the AG fault, the phase-A voltage is decreased and the phase-A current is significantly increased. The voltage and current of the phase-B and phase-C are also maintained at the values same as the ones at the steady state. For the current in  $\alpha\beta0$  framework, the alpha and zero components are increased but the beta component is not changed.

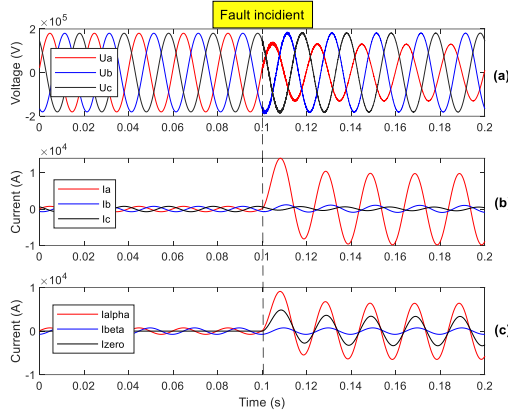


**Figure 10.** Fault simulation results at Source A: (a) Voltage waveform, (b) Current waveform in *abc* framework, (c) Current waveform in  $\alpha\beta0$  framework.

The proposed fault location method based on travelling wave using the DWT is performed by sampling the alpha component of the fault current at many frequencies to create the input data of the DWT. The level-1 detail coefficient of the DWT is then extracted to determine the arrival times of the reflected and forward waves at the beginning of the transmission line. The wavelet 1-D toolbox in MATLAB apps is used to analyse the alpha component of AG fault current in this case. The GUI of this toolbox is shown in Figure 11. These analysis results are an example for a AG fault at the location of 20km. The wavelet ‘db4’ is applied in this case. The level-1 detail and the details coefficients are displayed on the second and third plots in Figure 11. All these coefficients can be exported to the MATLAB workspace. Besides, the wavelet selection is performed by change it on the GUI. Therefore, this paper applies this wavelet toolbox to decompose the alpha component of the fault current for locating faults in a transmission line.

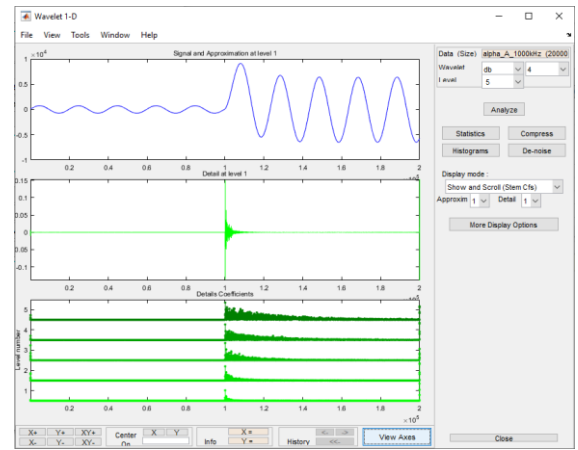


**Figure 11.** GUI of the wavelet 1-D toolbox.

To calculate the fault location, the propagation velocity of the travelling wave must be calculated based on the line parameters. The positive sequence line inductance and capacitance are used to determine the velocity  $v_{prop} = 1/\sqrt{LC} = 289942$  km/s.

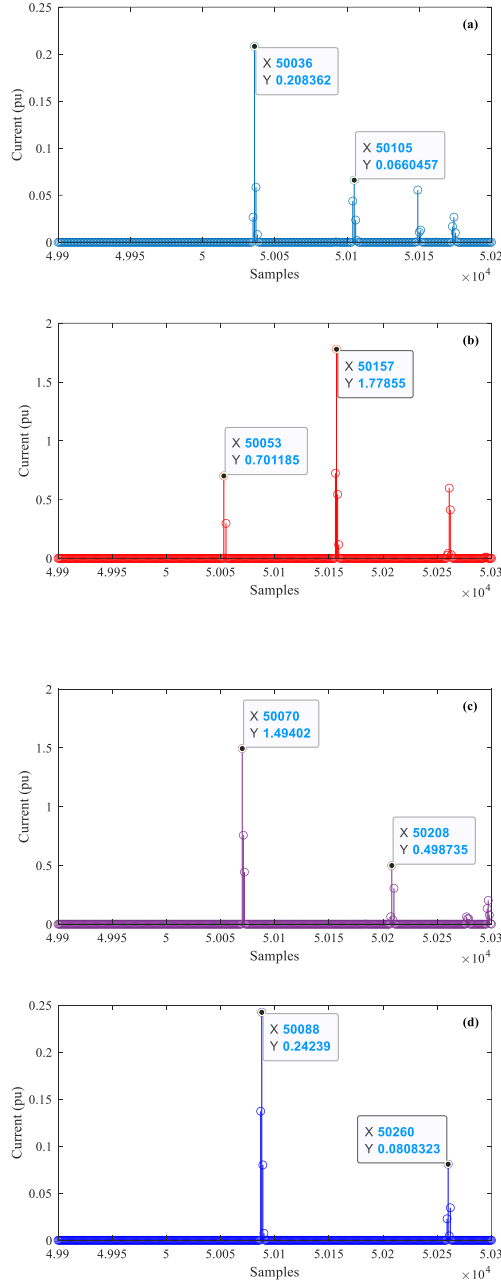
For the 20km-AG fault occurring at the time of 0.1 seconds, the level-1 detail coefficient of the DWT is analyzed as Figure 12(a) for the sampling frequency of 1000 kHz. From this figure, the index for the travelling wave from the fault location to the bus A is 50036 samples and the reflection wave from the fault location is 50105 samples. These indexes are multiplied by two and then plugging them into Eq. (8):

$$\begin{aligned} X &= \frac{1}{2}[(t_{A2} - t_A)v_{prop}] \\ &= \frac{1}{2}[(2 * 50036 - 2 * 50105) * 289942 \\ &\quad * \frac{1}{1000000}] = 20.01 \text{ km} \end{aligned}$$

Calculating the estimate error yields according to Eq. (25):

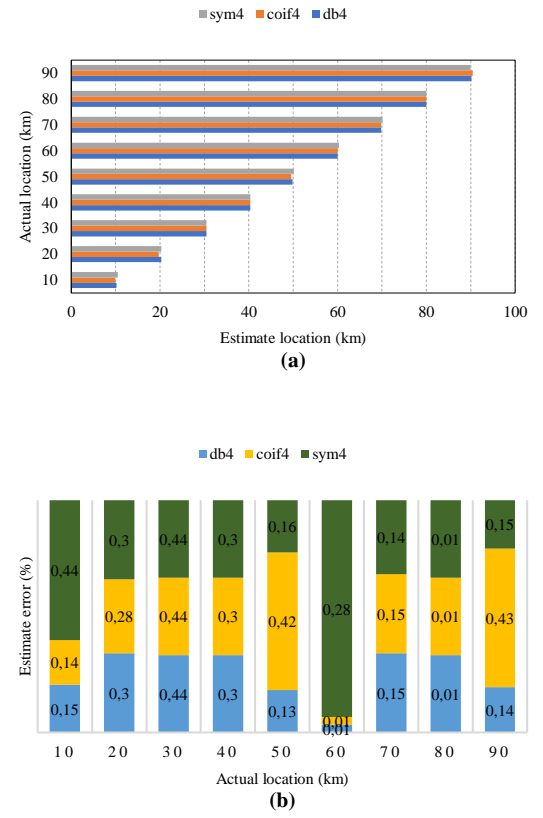
$$\begin{aligned} \text{Error}(\%) &= \left| \frac{L_{\text{estimate}} - L_{\text{actual}}}{L} \right| * 100 \\ \text{Error}(\%) &= \left| \frac{20.01 - 20}{100} \right| * 100 = 0.01\% \end{aligned}$$

The level-1 detail coefficients of the DWT for the 30km-AB, 40km-ABG, and 50km-ABCG faults for the sampling frequency of 1000 kHz are shown in Figures 12(b), (c), and (d), respectively. The indexes are clearly pointed on these figures to calculate the fault location on the transmission line. The estimate locations of three cases are 30.15 km, 40.01 km, and 49.87 km, respectively. As a result, the estimate errors of three cases are 0.15%, 0.01%, and 0.13%, respectively.

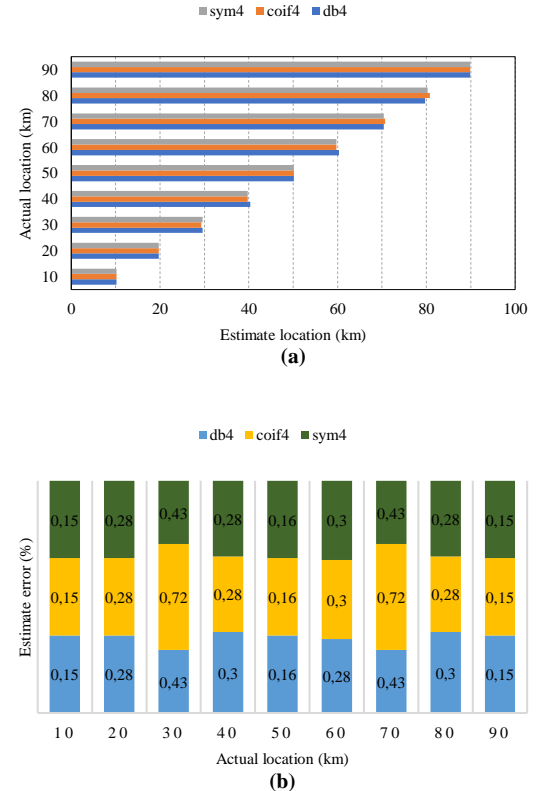


**Figure 12.** Level-1 detail coefficient, (a) 20km-AG fault, (b) 30km-AB fault, (c) 40km-ABG fault, (d) 50km-ABCG fault.

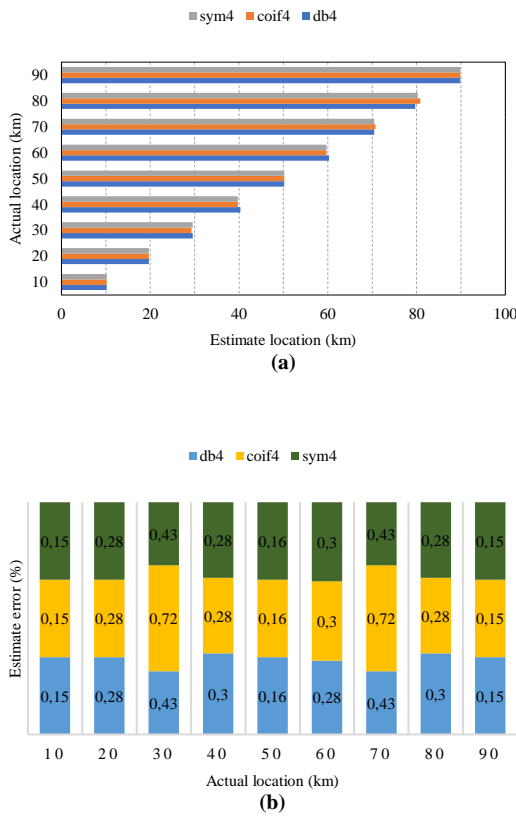
According to the above theory, the proposed fault location method was applied for many case studies in this paper to evaluate the effectiveness of the proposed method. The fault location was changed along the power transmission line. Additionally, the three wavelets including ‘db4’, ‘coif4’, and ‘sym4’ were applied to decompose the alpha component of the fault current. The estimate errors of the wavelets were compared as shown in Figure 13 for a single-phase-to-ground fault (AG), Figure 14 for a phase-to-phase fault (AB), Figure 15 for a double-phase-to-ground fault (ABG), and Figure 16 for a three-phase-to-ground fault.



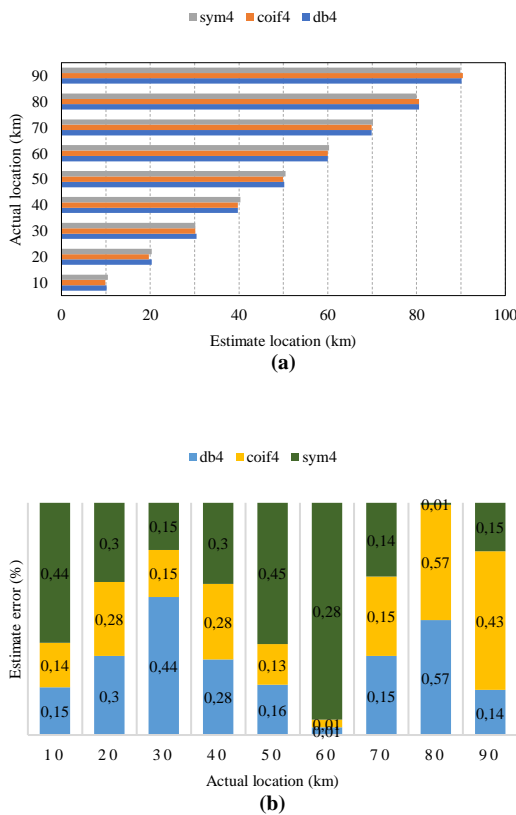
**Figure 13.** Simulation results of single-phase-to-ground fault, (a) Estimate location, (b) Estimate error.



**Figure 14.** Simulation results of phase-to-phase fault, (a) Estimate location, (b) Estimate error.



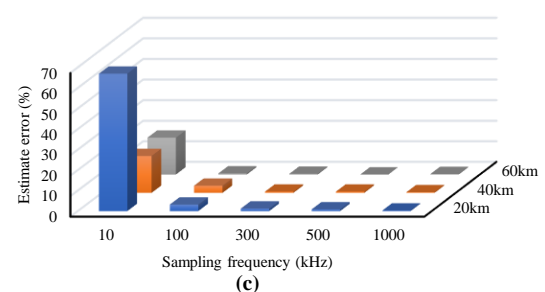
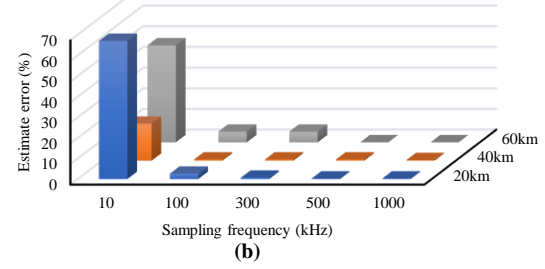
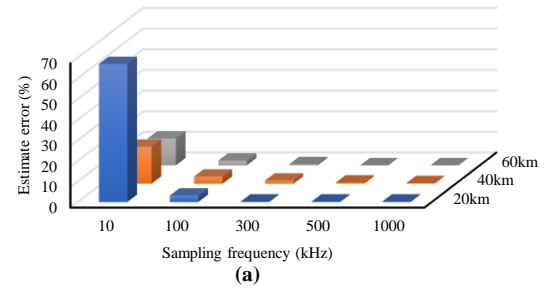
**Figure 15.** Simulation results of double-phase-to-ground fault, (a) Estimate location, (b) Estimate error.



**Figure 16.** Simulation results of three-phase-to-ground fault, (a) Estimate location, (b) Estimate error.

### 3.4. Sampling frequency comparison

In this case, the AG fault current waveforms at three locations (20, 40, and 60 km) are sampled at five different sampling frequency (10 kHz, 100 kHz, 300 kHz, 500 kHz, and 1000 kHz) to evaluate the performance of the proposed fault location method in this paper. These simulation results are presented in Figure 17. As shown in this figure, the dependances of the estimate error according to the sampling frequency which the wavelets ‘db4’, ‘coif4’, and ‘sym4’ are applied to extract the level-1 detail coefficient are shown in Figure 17(a), (b), and (c), respectively. In general, the estimate error will be decreased if the the sampling frequency is increased.



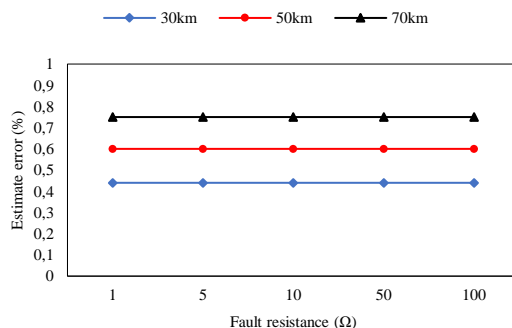
**Figure 17.** Estimate error according to sampling frequency, (a) wavelet ‘db4’, (b) wavelet ‘coif4’, (c) wavelet ‘sym4’.

Figure 17 compares the fault location results of the three wavelets using the single-ended method for a AG fault sampled at 10 kHz, 100 kHz, 300 kHz, 500 kHz, and 1000 kHz. The error of the 10 kHz sample frequency goes as high as 75.21% indicating an inadequate sampling

frequency for fault location. The sampling frequency requirement to get within 1000 m of the actual fault location begins at 300 kHz. The sampling frequency requirement to get within 100 m of the actual fault location requires at least 500 kHz. The sampling frequency requirement to get with 10 m of actual fault is seen only for 500 kHz and 1000 kHz for faults less than halfway of the total line length. It is obviously that the sampling frequency of 1000 kHz has the smallest estimate error in this study. Therefore, practical fault location systems are recommended to initialize their sampling frequency at the one to achieve a high estimate error.

### 3.5. Fault resistance comparison

As analysed in Introduction, the fault resistance will have impact on the estimate error of the impedance-based fault location methods. However the travelling wave-based fault location methods will have not been impact of the fault resistance. To demonstrate this issue, five different fault resistances including  $1\ \Omega$ ,  $5\ \Omega$ ,  $10\ \Omega$ ,  $50\ \Omega$ , and  $100\ \Omega$  are assumed for a AG fault occurring at the locations (30, 50 and 70 km). These simulation results are proved in Figure 18. It can be seen that Figure 18 compares the fault estimate error results of the three wavelets ('db4', 'coif4', 'sym4') using the single-ended method for the AG fault with various fault resistances. As a result, the estimate errors remain unchanged when increasing the fault resistance.



**Figure 18.** Estimate error according to fault resistance.

## 4. CONCLUSION

In this paper, a proposed method to locate faults accurately in a power transmission line was presented. The fault location method is based on single-ended travelling wave using the discrete wavelet transform to extract the level-1 detail coefficient from the fault current. The fault current at a single end of the transmission line is recorded and processed by the Clark transform and discrete wavelet transform to obtain the travelling wave signals and determine the

forward wave propagation and reflected waves generated by the fault.

The proposed method was tested using the test system of a single-circuit transmission line, and it was implemented in MATLAB/Simulink software. Several fault resistances and locations along the line were simulated to generate case studies and to evaluate the effectiveness of the proposed method. The simulation results show that the proposed method produce small errors, around 0.18% using the wavelet 'db4', around 0.24% using the wavelet 'coif4', and around 0.25% using the wavelet 'sym4'. It should be recommended that the travelling wave-based fault location method does not depend on the fault resistance.

The choice of the most suitable sampling frequency for locating faults in transmission lines was also investigated in this paper. It can be obviously observed from the mentioned simulation results that the estimated error results depend on the sampling frequency. Based on the obtained results, it is possible to design a fault location system with a high sampling frequency of 1000 kHz to achieve a high accuracy.

## REFERENCES

1. A. Mukherjee, P. K. Kundu, A. Das. Transmission line faults in power system and the different algorithms for identification, classification and localization: a brief review of methods, *Journal of The Institution of Engineers (India): Series B*, **2021**, 102, 855-877.
2. P. O. K. Anane, Q. Huang, O. Bamisile, P. N. Ayimbire. Fault location in overhead transmission line: A novel non-contact measurement approach for traveling wave-based scheme, *International Journal of Electrical Power & Energy Systems*, **2021**, 133, 107233.
3. A. Prasad, J. B. Edward, K. Ravi. A review on fault classification methodologies in power transmission systems: Part—I, *Journal of Electrical Systems and Information Technology*, **2018**, 5(1), 48-60.
4. H. A. Abd el-Ghany, A. M. Azmy, A. M. Abeid. A general travelling-wave-based scheme for locating simultaneous faults in transmission lines, *IEEE Transactions on Power Delivery*, **2019**, 35(1), 130-139.
5. S. Das, S. Santoso, A. Gaikwad, M. Patel. Impedance-based fault location in transmission networks: theory and application, *IEEE Access*, **2014**, 2, 537-557.
6. M. M. Hashim, H. W. Ping, V. K. Ramachandaramurthy. *Impedance-based fault*

*location techniques for transmission lines*, IEEE Region 10 Conference, Singapore, 2009.

7. N. M. Khoa, M. V. Cuong, H. Q. Cuong, N. T. T. Hieu. Performance comparison of impedance-based fault location methods for transmission line, *International Journal of Electrical and Electronic Engineering & Telecommunications*, **2022**, 11(3), 234-241.
8. J. Mora-Florez, J. Meléndez, G. Carrillo-Caicedo. Comparison of impedance based fault location methods for power distribution systems, *Electric Power Systems Research*, **2008**, 78(4), 657-666.
9. G. Ma, L. Jiang, K. Zhou, G. Xu. A Method of line fault location based on traveling wave theory, *International Journal of Control and Automation*, **2016**, 9(2), 261-270.
10. A. M. Elhaffar. *Power transmission line fault location based on current traveling waves*, Doctoral thesis, Helsinki University of Technology, 2008.
11. S. Lin, Z. Y. He, X. P. Li, Q. Q. Qian. Travelling wave time-frequency characteristic-based fault location method for transmission lines, *IET Generation, Transmission & Distribution*, **2012**, 6(8), 764-772.
12. D. Wang, J. Liu, M. Hou. Novel travelling wave fault location approach for overhead transmission lines, *International Journal of Electrical Power & Energy Systems*, **2024**, 155, 109617.
13. S. L. Zimath, J. A. P. Moutinho, L. B. de Oliveira, C. A. Dutra, J. H. M. de Resende, R. R. Matos. Traveling wave fault location applied to high impedance events, *12th IET International Conference on Developments in Power System Protection*, Copenhagen, Denmark, 2014.
14. D. Wang, M. Hou, Y. Guo. Travelling wave fault location of HVAC transmission line based on frequency-dependent characteristic, *IEEE Transactions on Power Delivery*, **2020**, 36(6), 3496-3505.
15. M. Aurangzeb, P. Crossley, P. Gale. Fault location on a transmission line using high frequency travelling waves measured at a single line end, *2000 IEEE Power Engineering Society Winter Meeting*, Singapore, 2000.
16. O. Naidu, A. K. Pradhan. Precise traveling wave-based transmission line fault location method using single-ended data, *IEEE Transactions on Industrial Informatics*, **2020**, 17(8), 5197-5207.
17. F. V. Lopes, K. M. Silva, F. B. Costa, W. L. A. Neves, D. Fernandes. Real-time traveling-wave-based fault location using two-terminal unsynchronized data, *IEEE Transactions on Power Delivery*, **2016**, 30(3), 1067-1076.
18. F. V. Lopes, K. M. Dantas, K. M. Silva, F. B. Costa. Accurate two-terminal transmission line fault location using traveling waves, *IEEE Transactions on Power Delivery*, **2017**, 33(2), 873-880.
19. M. Korkali, H. Lev-Ari, A. Abur. Traveling-wave-based fault-location technique for transmission grids via wide-area synchronized voltage measurements, *IEEE Transactions on Power Systems*, **2012**, 27(2), 1003-1011.
20. O. Naidu, A. K. Pradhan. A traveling wave-based fault location method using unsynchronized current measurements, *IEEE Transactions on Power Delivery*, **2019**, 34(2), 505-513.
21. Q. Jian, C. Xiangxun, Z. Jianchao. Travelling wave fault location of transmission line using wavelet transform, *International Conference on Power System Technology*, Beijing, China, 1998.
22. V. Gonzalez-Sanchez, V. Torres-García, D. Guillen. Fault location on transmission lines based on travelling waves using correlation and MODWT, *Electric Power Systems Research*, **2021**, 197, 107308.
23. D. T. Viet, N. H. Hieu, N. M. Khoa. A method for monitoring voltage disturbances based on discrete wavelet transform and adaptive linear neural network, *International Review of Electrical Engineering*, **2016**, 11(3), 314-322.
24. L. Zhan, Y. Liu, Y. Liu. A Clarke transformation-based DFT phasor and frequency algorithm for wide frequency range, *IEEE Transactions on Smart Grid*, **2016**, 9(1), 67-77.